Simulation and Prediction of Soil Erosion in Daning River Basin

Wenqian Bai, Huiru Hu, Li He, Zhengwei He, and Yang Zhao

***Abstract*—Calculating soil erosion intensity and predicting its change trend is essential for the precise implementation of control measures. We had estimated and quantitatively analyzed the current situation of soil erosion in the Daning River Basin in 2008, 2013, and 2018 using the revised universal soil loss equation model. We also analyzed the correlation between distance from the river, elevation, and slope, followed by the analysis and prediction of the soil erosion in the Daning River Basin in 2023 by constructing a cellular automaton (CA)-artificial neural network (ANN)-Markov model. The results demonstrated the total soil erosion to be 798.49, 746.38, and 628.78 10^4 t in 2008, 2013, and 2018, respectively. The overall trend of soil erosion was found to be decreasing and the spatial distribution of soil erosion was strongly correlated with the distance from the river, elevation, and slope. Based on the CA-ANN-Markov model prediction, the trend of soil erosion from 2018 to 2023 is consistent with that from 2008 to 2013. Light, moderate, and intense erosion demonstrated an increasing trend, whereas slight, very intense, and intense erosion demonstrated a decreasing trend. By estimating and predicting soil erosion in the Daning River Basin, this article provides a reference for ecological restoration and the control of soil erosion in small watersheds under similar environments.**

***Index Terms*—Cellular automaton (CA)-artificial neural network (ANN)-Markov, Daning River Basin, quantitative evaluation, revised universal soil loss equation (RUSLE), soil erosion.**

I. Introduction

SOIL erosion has caused serious impacts on the current global ecosystem security and protection systems [1], [2]. Soil erosion leads to an imbalance in soil stability while causing beneficial nutrient loss essential for crop growth [3], [4]. The eutrophication of water resources exacerbated by the nitrogen and phosphorus carried in the produced sediment [5], [6] also poses a threat to water resources security and may lead to droughts [7]. At the same time, a large amount of sediment produced by erosion enter the water body, which not only pollutes the watershed [8] but also its accumulation causes siltation and elevation of the riverbed. Moreover, it could lead to the occurrence of flood hazards [9] and seriously endanger urban safety [10]. Soil erosion as an environmental problem could seriously affect ecological quality. Therefore, it is the focus of current environmental protection work and a hot spot for research.

Numerous models are available for the assessment of regional soil erosion. Among them, assessment models can be divided into two main categories. One is the physical-based process model, such as the Water Erosion Prediction Project (WEPP) [11] and the European Soil Erosion Model [12], which require large amounts of measured data and are difficult to implement in large-scale areas. The other is empirical models such as soil loss equation (USLE) [13], modified USLE (MUSLE) [14], and the revised universal soil loss equation RUSLE [15]. The USLE, which was adopted in the 1830s and 1840s [13], is more widely used. However, it has drawbacks such as overestimation of soil erosion on low-erosion plots and underestimation of predictions for high-erosion plots [16], [17]. It is only suitable for gentle sloping areas rather than areas with high complex slopes [18]. Based on this, the MUSLE [14] was proposed to solve this problem. The rainfall factor is replaced by a runoff factor and the hydrological procedure for sand production prediction is optimized. The MUSLE was developed for specific field conditions and its application without calibration could lead to a large number of errors. Therefore, the original USLE has been revised again as the revised universal soil loss equation (RUSLE) [19] but was improved based on experimental data, algorithms, theoretical interpretations of different landforms, soil types, land use types, soil conservation measures, and climatic factors compared to traditional studies [20]–[22]. RUSLE added the ability in USLE to process crops correctly. RUSLE can more efficiently handle nonuniform slopes (concave and convex slopes) [23], [24]. The modified RUSLE model has relatively high accuracy and applicability. Therefore, it is gradually being used worldwide for soil erosion estimation [25]. Meanwhile, with the emergence of geographic information system (GIS) and remote sensing (RS) technologies, large-scale studies on soil erosion can be performed [26]–[28]. Current research applications of RUSLE's model are dedicated to the subdivided geospatial regions and special environmental conditions for soil erosion prediction [29]–[31], with further improvements

Manuscript received April 15, 2022; revised May 26, 2022; accepted June 6, 2022. Date of publication June 10, 2022; date of current version June 29, 2022. This work was supported in part by the Natural Science Foundation of Sichuan, China under Grant 2022NSFSC1040, in part by the Independent Research Project of the State Key Laboratory of Geohazard Prevention and Geoenvironment Protection Independent Research Project under Grant SKLGP2021Z003. *(Wenqian Bai and Huiru Hu contributed equally to this work.) (Corresponding author: Li He.)*

Wenqian Bai, Huiru Hu, Zhengwei He, and Yang Zhao are with the State Key Laboratory of Geohazard Prevention and Geoenvironment Protection, Chengdu University of Technology, Chengdu 610059, China, and also with the College of Earth Sciences, Chengdu University of Technology, Chengdu 610059, China (e-mail: baiwenqian@stu.cdut.edu.cn; 1094962069@qq.com; hzw@cdut.edu.cn; byteyang@foxmail.com).

Li He is with the State Key Laboratory of Geohazard Prevention and Geoenvironment Protection, Chengdu University of Technology, Chengdu 610059, China, and also with the College of Tourism and Urban-Rural Planning, Chengdu University of Technology, Chengdu 610059, China (e-mail: heli2020@cdut.edu.cn).

Digital Object Identifier 10.1109/JSTARS.2022.3181885

in modeling accuracy and applicability [20]. The above studies mostly optimized the model structure and improved the parameters. However, there are relatively few studies on time-scale prediction while considering the complex ecological and geological environment under the pressure of mountainous watershed topography. Moreover, the Three Gorges Reservoir (TGR) storage made it difficult to accurately evaluate and predict the soil erosion in the Daning River Basin. Therefore, using a reasonable evaluation system and selecting suitable evaluation factors for the accurate evaluation of soil erosion in the area are important for the development of soil and water conservation work.

This article proposes to use a prediction model of soil erosion consisting of three parts: the cellular automaton (CA) model [32], the artificial neural network (ANN) model [33], and the Markov model [34]. The CA model is a complete tool for soil erosion change analysis, which can obtain the change trends predicted by soil erosion and the conversion rules of soil erosion through ANN, which in turn simplifies CA to define the conversion rules [35]. Markov can calculate the change in the transition probability matrix of soil erosion type in two periods, which can be used to predict the direction and the change in the amount of soil erosion intensity in a certain period [36]. This study benefits from the advantages of the three models to construct a CA-ANN-Markov model.

In recent years, research has been conducted across the world on the process of soil erosion generation and the interaction between some influencing factors [37]–[39], which has made significant progress and promoted research on the process of soil erosion. However, uncertainty is still existing in estimating the values of soil erosion loss. In-depth research and improvement are required to resolve problems and shortcomings in soil erosion research [40]. In the RUSLE model, the traditional extraction of the cover management factor (C) is obtained by NDVI from RS images. Moreover, the default image element is uniformly distributed internally and the details of surface information are not effectively considered. In the previous quantitative soil erosion analysis, the data were limited to the previous years for soil erosion evaluation, which was not time-sensitive and could not propose future planning solutions for soil erosion management measures. The CA-ANN-Markov model has been applied in urban dynamic change prediction and its accuracy has been widely verified [41], [42]. However, its application and the ability of prediction in areas such as soil erosion prediction are yet to be verified in depth.

This article assessed and predicted the soil erosion changes in the Daning River Basin. Based on RS images and hydrological information data, the RUSLE model combined with GIS and RS technology was used to estimate soil erosion in the Daning River Basin. The spatial and temporal variation characteristics of its soil erosion and the driving effects of influencing factors were also analyzed. A CA-ANN-Markov soil erosion prediction model was constructed to predict the future soil erosion trends. This study intended to address the following issues:

1) improving the accuracy of the vegetation cover management C-factor based on the hybrid image element decomposition method;
2) application of the CA-ANN-Markov model to evaluate and predict soil erosion in the Daning River Basin and demonstrating the feasibility of this model in areas with complex geomorphic environments;
3) exploring the current situation of soil erosion in the watershed, predicting its change trend, providing a reliable theoretical basis and data support for the ecological protection as well as management of the watershed.

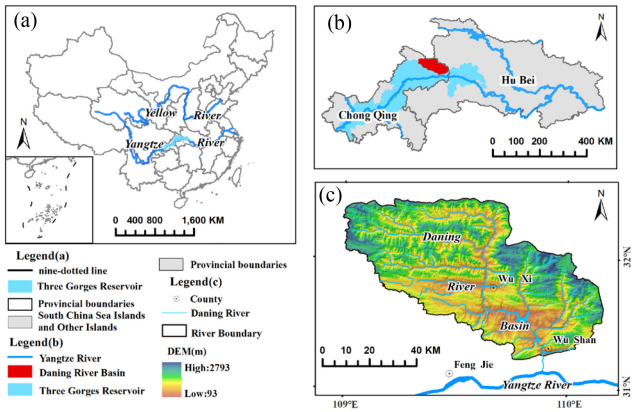

Fig. 1. (a) Location of TGR Area in China. (b) Location of the Daning River in the TGR Area. (c) Topographic features of the Daning River.

II. Data and Method

A. Study Area

The Daning River Basin is located in the core of the TGR area of the Yangtze River. It is one of the key inundation areas, which belongs to Chongqing with a total basin area of 4482 km^2, a distribution range of 108°44′E to 110°11′E and 31°04′N to 31°44′N and a total length of about 250 km (see Fig. 1). According to the National Bulletin of Soil and Water Conservation data 2020 [43], the area of soil erosion in the TGR was 18 800 km^2, accounting for 32.57% of the total land area (57 700 km^2). The type of soil erosion was mainly hydraulic erosion. The Daning River is located in the arc-shaped fold belt of the Daba Mountain and the geomorphology is characterized by mountainous terrain in the high northeast and low southwest. It has large altitude differences and regional differences resulting in vertical zonal distribution of soils. The brown loam is dominant in high-altitude alpine mountains, yellow-brown loam, and yellow loam are dominant in middle-altitude mountains, and rice soil and purple soil are dominant in low-altitude river valley areas. These soil types are highly susceptible to erosion [44]. The study area belongs to the north subtropical monsoon climate, with the average annual temperature around 18°C. Rainfall is mostly concentrated in summer while having mostly acidic rainstorms, which makes soil erosion extremely easy to occur. At the same time, the unreasonable setting of agricultural land in the Daning River Basin, the destruction of vegetation, the reconstruction of projects, and natural disasters have caused different degrees of soil erosion. The study can evaluate the current situation of soil erosion in the Daning River Basin and predict the future development trend, which has implications for the protection of the Yangtze River ecological barrier.

B. Data

The data required in this study included precipitation, soil type, RS, and land use type.

RS data included vegetation, land cover, and elevations. RS images used in vegetation cover and land use data were obtained from the official website of the United States Geological Survey.[1] The Landsat images (spatial resolution: 30 m) were selected for the three years (2008, 2013, and 2018) having low cloudiness in the Daning River Basin. The raw Landsat images were preprocessed. Based on the hybrid image element decomposition, vegetation cover data were obtained. Subsequently, the data were mainly used for the calculation of the vegetation cover management (C) factor (spatial resolution: 30 m). The vegetation cover data were classified and visually interpreted to obtain the type of land use data. The classification results were evaluated by Kappa for accuracy and land use accuracy of 85% and above was achieved. It was primarily used for the calculation of the soil and water conservation (P) factor (spatial resolution: 30 m).

Elevation image data with a resolution of 30 m were obtained from the geospatial data cloud[2] and preprocessed via ArcGIS for the projection transformation and cropping. It was mainly used for the subsequent calculation of the slope length slope steepness (LS) factor and CA-ANN-Markov model prediction.

The 1:1 million soil type and texture data were obtained from the Resource and Environmental Science and Data Center.[3] The mapping units used for this data included soil class, subclass, soil genus, and soil species. Eight soil classes were involved in this study area. The data were used for the calculation of soil erodibility factor K (spatial resolution: 30 m).

The daily precipitation data were obtained from the China Meteorological Data Network.[4] There are 13 stations around the Daning River Basin. The monthly precipitation and total annual precipitation of each station need to be calculated. The Wischmeier WH method [13] was used to calculate the *R*-value of each station and the kriging interpolation method was used to obtain the 30-m rainfall erosion force R-value.

This article unified the spatial resolution to 30 m×30 m for precipitation and soil data. Among them, direct kriging interpolation of precipitation data decreases the median *R*-factor while making soil erosion lower [45]. However, during *R*-factor estimation, Kumar *et al.* [46] showed that kriging interpolation produced the lowest error in all periods regardless of the number of gauges and image element size used for interpolation. Direct downscaling of soil data results in attribute and geometric errors.

C. Method

To restore eroded soils and reduce erosion risk, innovative strategies with a good understanding of the location, extent of erosion rates, and future trends are required, which depends mainly on the use of sound input data and scientifically efficient processing models [45]. By inputting geomorphic and hydrological environmental factors affecting soil erosion into the CA-ANN-Markov model, the degree of influence of each factor on soil erosion and the current status of erosion can be assessed. Subsequently, the future development trend can be predicted so that detailed spatial maps can be generated directly, followed by the extraction of statistical information, which can solve the soil erosion prediction problem for similar soil erosion assessment and prediction research. Fig. 2 shows the method involved in this study.

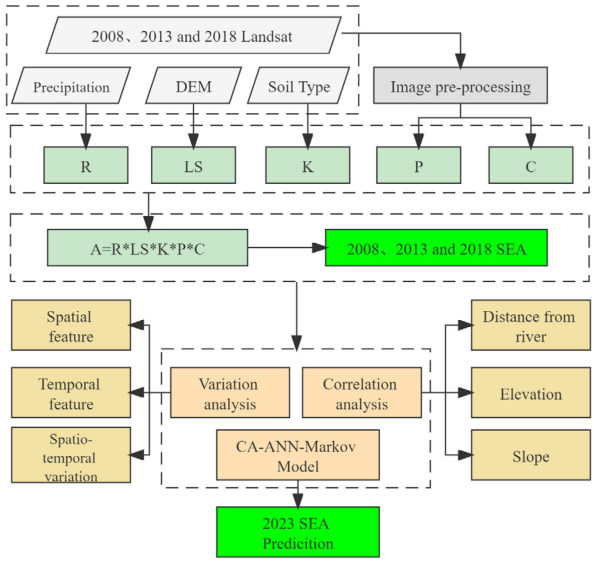

Fig. 2. Methodology of the study (all factors and abbreviations are defined in the text).

D. RUSLE

RUSLE model is mainly used to simulate soil loss on slopes, which is based on an empirical spatial set. The model is implemented to calculate soil loss on this basis. The expression of the RUSLE model is as follows:

$$A = R \times K \times \mathrm{LS} \times C \times P \tag{1}$$

where A represents the annual average soil erosion modulus (t/(hm^{2}a), R represents the rainfall erosion force factor (MJ·mm/(hm^{2}h·a)), K is the soil erodibility factor (t·h·hm^2/(hm^{2}MJ·mm)), L is the slope length, S is the slope steepness, C represents the vegetation management factor, and P represents the soil and water conservation measure factor, which is dimensionless and measures the field engineering protection and soil tillage.

The classical method [47] was selected to calculate the *R*-value of rainfall erosion force. The spatial distribution of the *R*-factor for 2008 [see Fig. 3(a)], 2013 [see Fig. 3(b)], and 2018 [see Fig. 3(c)] were obtained by interpolating the rainfall erosion force factor by Kriging. The hybrid image element decomposition method was utilized to calculate the *C*-value of cover management and the spatial distribution of the *C*-factor for 2008 [see Fig. 3(d)], 2013 [see Fig. 3(e)], and 2018 [see Fig. 3(f)] were obtained. Based on the study of Liu *et al.* [48] and considering the special situation of the watershed and construction land, the *P*-value was determined. Subsequently, the spatial distribution of the *P*-factor for 2008 [see Fig. 3(g)], 2013 [see Fig. 3(h)],

[1][Online]. Available: https://www.usgs.gov/
[2][Online]. Available: http://www.gscloud.cn/
[3][Online]. Available: https://www.resdc.cn/
[4]Accessed: Dec. 31, 2018. [Online]. Available: http://data.cma.cn/

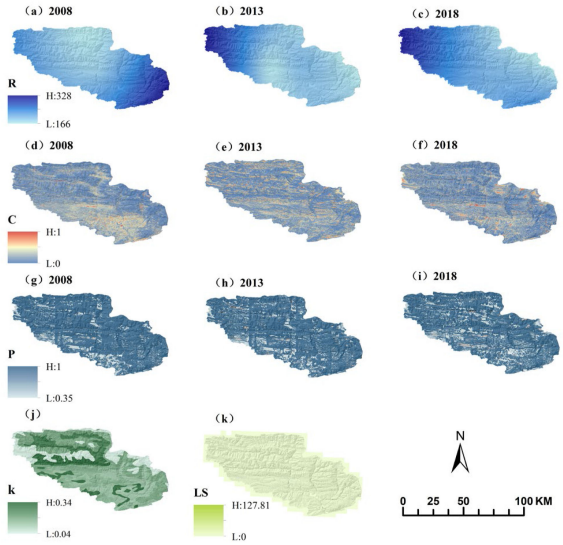

Fig. 3. RUSLE factor.

and 2018 [see Fig. 3(i)] were obtained. Soil data from the national secondary census results were used to assign values to the subclass properties. The generated *K* factor was shown in Fig. 3(j). The slope and slope length index calculation formula was based on the report of Liu *et al.* [49] and Zhang *et al.* [50], respectively. The final LS value was shown in Fig. 3(k).

E. CA-ANN-Markov Model

1) CA-ANN-Markov Model Construction: Soil erosion is a continuous change process. The formation of soil erosion is dependent on the spatial pattern change contributed by a variety of complex factors.

The CA model consists of five parts, which are tuple, tuple space, tuple neighborhood, transformation rule, and time. The ANN can adjust the relationship between nonlinear mappings by internal structure. The ANN itself is characterized by flexible learning and the processing and analysis of data with noise. The combination of ANN and CA can adjust the relationship between arbitrary nonlinear mappings by using an ANN with an internal structure chain. The advantage of using ANN includes the utilization of multiple influence factors which can derive the transformation rules of CA and simulate the change of soil erosion. By establishing a relationship between the influence factors and the transformation probability, the weight of each factor influenced by human factors is avoided while predicting soil erosion more accurately and reasonably. The difference between the CA model and the Markov model is that the CA model can simulate the prediction of microlocal changes, while Markov can control the changes of soil erosion macroscopically. Markov model is based on the number and direction of transformation between different soil erosion intensities, which predicts the overall development trend using a probability matrix.

By combining CA, ANN, and Markov to construct the CA-ANN-Markov prediction model, the prediction effect and accuracy could be improved because of the strong spatial prediction ability of the meta-automaton model and the advantage of the Markov model.

2) CA-ANN-Markov Model Validation: The CA-ANN-Markov model requires soil erosion results as well as impact factor data to predict soil erosion. To validate the model accuracy and avoid the shortcomings of overestimating traditional validation (e.g., Kappa coefficient) [51], this study uses the figure-of-merit (FoM) index to validate the model feasibility while referring to the previous report [52] simultaneously. The corresponding calculations are presented in the following equations:

$$\text{FoM} = \frac{B}{A+B+C+D} \tag{2}$$

$$\text{Product's accuracy (PA)} = \frac{B}{A+B+C} \tag{3}$$

$$\text{User's accuracy (UA)} = \frac{B}{B+C+D} \tag{4}$$

where A denotes the actual conversion and simulation of the number of unconverted image elements, B represents the actual conversion and simulation of the number of error-free image elements, C represents the actual change and simulation of the wrong-type conversion image elements, and D represents the actual unconverted and simulation of the number of converted image elements.

A comprehensive analysis of the basic situation of the Daning River Basin revealed that the basin had complex terrain, fragmented topographic and geomorphological patterns, high vegetation cover, and complex and diverse vegetation types. Moreover, the populated geographic locations are distributed on both sides of the river. The six digital elevation model (DEM), normalized difference vegetation index (NDVI), precipitation, distance from the river, distance from the road, and population influence factor in 2018 were selected as the driving factors for this prediction and normalization. At first, the soil erosion transformation rules were mined by the CA-ANN-Markov model while considering 2008 as the starting year and 2013 as the ending year. The soil erosion condition in 2018 was predicted while selecting 2013 as the starting year. Based on the accuracy verification module, the predicted soil erosion intensity in 2018 was verified with the accuracy of the derived soil erosion intensity in 2018. After satisfying the accuracy requirements, soil erosion for 2023 was predicted. The normalized predictors, suitability matrix, and parameter settings were as per the previous parameters.

F. Analysis of Spatial and Temporal Variation

Soil erosion change over time is a complex process. A certain soil erosion intensity can be transformed which is from the other five categories of soil erosion intensity. Comparing the numerical increase and decrease relationship of soil erosion between different years, it is difficult to understand the changing pattern of soil erosion intensity and the dynamic change process between each erosion intensity. Therefore, the combination of the matrix transfer between soil erosion classes was chosen [53] for analysis. The basic mathematical form of the transfer matrix

TABLE I
SOIL EROSION GRADE INTENSITY DIVISION

Classes	SEM[t/(km^{2}a)]	MSEM[t/(km^{2}a)]	Average loss thickness(mm)
Slight	<500	250	<0.4
Minor	500-2500	1500	0.4-2.0
Moderate	2500-5000	3750	2.0-4.0
Intense	5000-8000	6500	4.0-6.4
Very intense	8000-15000	11500	6.4-12.0
Extreme	>15000	-	>12.0

Note: "SEM" is the soil erosion modulus, "MSEM" is the median soil erosion modulus.

is as follows:

$$S_{ij} = \begin{bmatrix} S_{11} & S_{12} & S_{13} & \cdots & \cdots & S_{1n} \\ S_{21} & S_{22} & S_{23} & \cdots & \cdots & S_{2n} \\ \cdots & \cdots & \cdots & \cdots & \cdots & \cdots \\ \cdots & \cdots & \cdots & \cdots & \cdots & \cdots \\ \cdots & \cdots & \cdots & \cdots & \cdots & \cdots \\ S_{n1} & S_{n1} & S_{n1} & \cdots & \cdots & S_{nn} \end{bmatrix} \quad (5)$$

where S refers to the area of each soil erosion intensity, n refers to the total number of soil erosion intensity types, i refers to the soil erosion intensity types in the early part of the study, j refers to the soil erosion intensity types in the later part of the study, and S_{ij} refers to the area of transfer of soil erosion intensity type i in the early part to soil erosion intensity type j in the latter part of the study.

G. Classifying Soil Erosion Intensity for Grading

Referring to the Chinese Ministry of Water Resources [54] and the water erosion intensity grading standard, the grading was made for different soil erosion intensities (see Table I). Considering the geographical characteristics of the Daning River Basin, the degree of soil erosion was expressed abstractly while using the rules of its grading. The degradation of land was judged according to the grading of soil erosion intensity. Subsequently, the ecological evaluation was carried out. The soil erosion results of the Daning River Basin in 2008, 2013, and 2018 were reclassified to obtain the classification results of soil erosion intensity for three years.

H. Soil Erosion Index (SEI)

Soil erosion can be decided by the magnitude of the SEI. The degree of soil erosion is produced by a combination of several factors. In this article, the calculation model of SEI was adopted to obtain the specific erosion characteristics. The comprehensive index of soil erosion (INDEX) proposed by Yang [55] was adopted, which can be expressed as follows:

$$\text{INDEX} = \sum_{i=1}^{n} W_i \, A_i \quad (6)$$

where INDEX refers to the integrated SEI, W_i refers to the value of the ith soil erosion intensity class, and A_i refers to the ratio of the area of the ith class to the value of the total area. The grading of soil erosion degree was classified as 0 (Slight), 2 (Minor), 4 (Moderate), 6 (Intense), 8 (Very Intense), and 10 (Extreme). Higher values represent higher INDEX impact for that grade, more intense soil erosion, and more severe erosion conditions to which the soil is subjected.

TABLE II
CHANGES IN EROSION WITH DIFFERENT EROSION INTENSITIES FROM 2008 TO 2018

Classes	2008(Year)		2013(Year)		2018(Year)	
	SEA (10^4 t)	SEM t/(km^{2}a)	SEA (10^4 t)	SEM (t/(km^{2}a))	SEA (10^4 t)	SEM (t/(km^{2}a))
Slight	4.71	19.24	4.98	18.56	5.23	22.08
Minor	175.14	1589.50	144.68	1434	172.18	1443.50
Moderate	240.89	5015.79	170.39	4277.07	213.03	3495.65
Intense	174.87	6233.30	133.50	7333.29	131.02	6192
Very intense	150.75	10336.28	188.26	11698.35	90.62	10174.97
Extreme	52.13	18758.36	104.57	19316.34	16.70	17529.68
Total	798.49	41952.47	746.38	44077.61	628.78	38857.88

Note: "SEA" is soil erosion amount,"SEM" is the soil erosion modulus.

III. RESULTS AND ANALYSIS

A. Soil Erosion Spatial Variation Features

After unifying the projection coordinate system for each factor raster data, each raster data was multiplied together with the RUSLE model using the raster calculator in ArcGIS to obtain the spatial distribution maps of different erosion intensities in the Daning River Basin in 2008, 2013, and 2018 (see Fig. 4).

Based on the analysis, soil erosion was found to be more common in the study area due to the special geographical location, complex mountainous terrain, and large variation of precipitation in the Daning River Basin. Soil erosion from 2008 to 2018 demonstrated a consistent spatial distribution, with a large proportion of microerosion, which was distributed throughout the region. These areas have higher vegetation cover, denser distribution of woodlands, and less human disturbance. Light erosion and moderate erosion are mainly distributed in the central area of the Daning River Basin, where soil fertility decreases under the action of hydraulic erosion coupled with unreasonable land development. In the Miaotang, Danyang, Shuangyang, and Lanying Village, intense erosion and very intense erosion could be found. As the above areas are having low vegetation cover, rough cultivation, high human activities, and frequent occurrence of geological disasters, the presence of high-intensity soil erosion is common.

B. Soil Erosion Temporal Variation Features

The SEM was calculated for 2008, 2013 and 2018 in the Daning River Basin by the RUSLE model based on R, K, LS, C and P factors. The results of the variation of erosion at different erosion intensities (see Table II) were calculated according to the criteria for grading soil erosion intensity (see Table I). The statistical analysis was performed to obtain the area share data of different erosion intensities from 2008 to 2018 (see Table III).

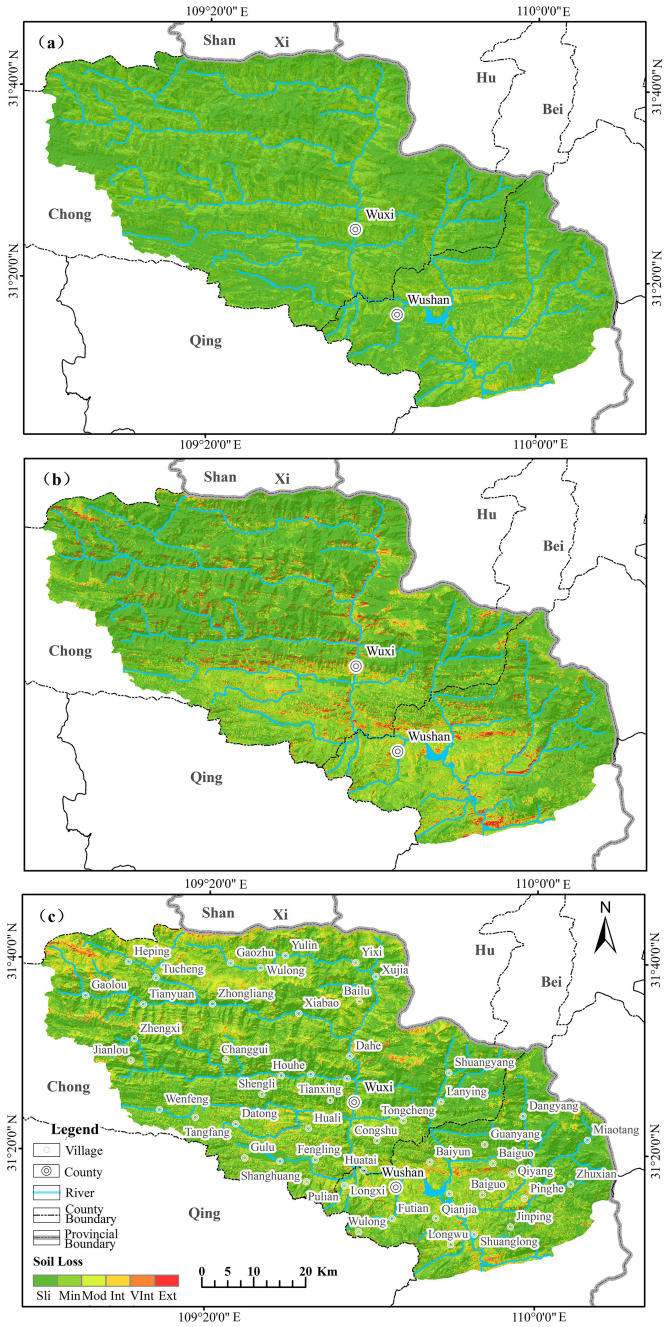

Fig. 4. Spatial distribution of soil erosion in 2008, 2013, and 2018. Note: Sli indicates that the soil erosion level is slight, Min indicates that the soil erosion level is minor, Int indicates that the soil erosion level is intense, VInt indicates that the soil erosion level is very intense, and Ext indicates that the soil erosion level is extreme.

As presented in Table II, the total soil erosion in 2013 was found to be significantly smaller than in 2008, which indicated that the overall soil erosion decreased from 2008 to 2013. Comparing 2013 and 2018, the value of total soil erosion in 2018 was determined to be significantly smaller than in 2013, which indicated a decreasing trend of overall soil erosion from 2013 to 2018. As can be seen from Table IV, during the 2008-2018 period, the erosion area of the slight, very intense and intense grades showed an increasing, followed by decreasing trend.

TABLE III
CHANGE IN THE AREA WITH DIFFERENT EROSION INTENSITIES FROM 2008 TO 2018

Classes	2008(Year)		2013(Year)		2018(Year)	
	EA (km^2)	AP (%)	EA (km^2)	AP (%)	EA (km^2)	AP (%)
Slight	2445.44	54.56	2681.54	59.83	2369.41	52.87
Minor	1101.88	24.59	1004.74	22.42	1192.77	26.61
Moderate	480.26	10.72	398.38	8.89	609.40	13.6
Intense	280.55	6.26	182.05	4.06	211.59	4.72
Very intense	145.85	3.25	160.93	3.59	89.07	1.99
Extreme	27.79	0.62	54.14	1.21	9.53	0.21
Total	4481.76	100	4481.76	100	4481.76	100

Note: "EA" stands for erosion area and "AP" stands for area percentage.

TABLE IV
SOIL EROSION INTENSITY AREA TRANSFER MATRIX FROM 2008 TO 2013

2008(Year)	ratio/ area	2013(Year) Slight	Minor	Moderate	Intense	Very intense	Extreme
Slight	ratio	77.28	16.97	3.63	1.16	0.77	0.19
	area	1889.75	415.04	88.79	28.39	18.83	4.65
Minor	ratio	52.37	30.51	11.35	3.58	1.93	0.27
	area	577.05	336.13	125.09	39.44	21.25	2.92
Moderate	ratio	31.57	31.69	18.61	9.08	7.28	1.77
	area	151.63	152.19	89.39	43.60	34.96	8.50
Intense	ratio	17.21	26.32	22.65	14.78	14.35	4.69
	area	48.29	73.85	63.53	41.47	40.25	13.16
Very intense	ratio	8.99	16.73	19.59	17.92	25.70	11.08
	area	13.11	24.40	28.57	26.13	37.48	16.16
Extreme	ratio	6.19	11.29	10.81	10.85	29.35	31.52
	area	1.72	3.14	3	3.02	8.16	8.76

Note: Ratio (%), Area (km^2).

Whereas, the erosion area of the minor, moderate and intense grades showed a decreasing followed by an increasing trend.

Comparing the yield of 2008 with 2018, an overall decrease trend in soil erosion and an improvement in soil erosion was found.

C. Spatial and Temporal Variation of Soil Erosion

To specifically analyze the transformation of each soil erosion intensity in the Daning River Basin, the spatial analysis of soil erosion intensity based on the RUSLE model for three years (2008, 2013, and 2018) was carried out separately. The area matrix of soil erosion intensity transferred from 2008 to 2013 (see Table IV) and 2013 to 2018 (see Table V) in the Daning River Basin was statistically obtained.

TABLE V
SOIL EROSION INTENSITY AREA TRANSFER MATRIX FROM 2013 TO 2018

2013(Year)		2018(Year)					
	ratio/area	Slight	Minor	Moderate	Intense	Very intense	Extreme
Slight	ratio	67.13	21.27	8.89	2.15	0.51	0.04
	area	1800.23	570.44	238.33	57.77	13.59	1.19
Minor	ratio	29.49	47.65	17.62	3.95	1.15	0.14
	area	296.31	478.80	176.99	39.68	11.57	1.39
Moderate	ratio	33.54	25.25	26.88	10.60	3.49	0.25
	area	133.61	100.57	107.09	42.21	13.90	0.99
Intense	ratio	36.06	15.18	24.98	16.30	7.03	0.46
	area	65.64	27.63	45.47	29.67	12.79	0.84
Very intense	ratio	35.07	8.42	21.18	19.89	14.30	1.13
	area	56.44	13.55	34.09	32.01	23.01	1.83
Extreme	ratio	31.72	3.28	13.74	18.94	26.24	6.07
	area	17.18	1.78	7.44	10.26	14.21	3.29

Note: Ratio (%), Area(km^2).

Considering the RUSLE model and the 2008–2013 period, the slight soil erosion was transformed into minor erosion while having a transformed ratio of 16.97 (see Table IV). The minor erosion was converted to slight erosion while having a transformed ratio of 52.37. The most moderate erosion conversions were found to be slight erosion and minor erosion, having conversion ratios of 31.57 and 31.69. The intense erosion was transformed into minor and moderate erosion while resulting in a transformed ratio of 26.32 and 22.65, respectively. The very intense erosion area was found to be comparatively less, which predominantly transformed into minor, moderate and intense erosion, with a transformation ratio of 16.73, 19.59, and 17.92, respectively. The area of extreme erosion was determined to be less and a small portion of the severe erosion was transformed outward. Overall, the erosion was mainly transformed to the adjacent erosion intensity. Most of the areas demonstrated a decreasing erosion trend while only a few areas were transformed into areas having increased erosion.

The slight erosion was transformed into minor erosion from 2013 to 2018, resulting in a transformation ratio of 21.27 (see Table V). Minor erosion converted mainly to slight erosion, with a transformation ratio of 29.49. Moderate erosion transformed mostly into slight erosion, with a transformation ratio of 33.54. Intense erosion was mainly transformed into slight erosion, with a transformation ratio of 36.06. Very intense erosion was transformed into slight erosion, with a transformation ratio of 35.07. The extreme erosion was mainly transformed into slight erosion, with a transformation ratio of 31.72. As a whole, erosion was mainly transformed to the adjacent erosion intensity. Most of the areas demonstrated a decreasing erosion trend while only a few areas transformed into areas having increased erosion.

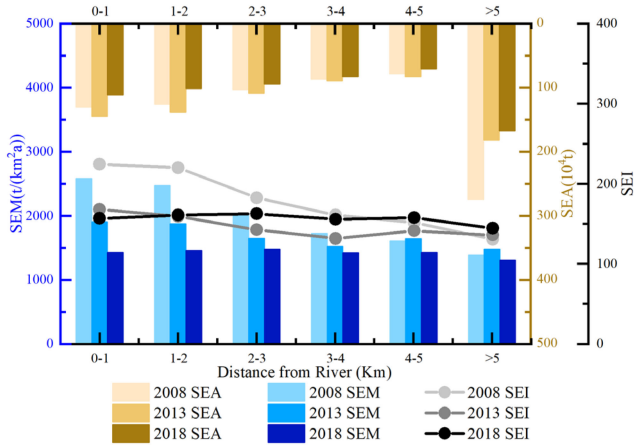

Fig. 5. Variation of SEA, SEM, and SEI with time at different distances from the river. Note: SEA is soil erosion amount, SEM is soil erosion modulus, and SEI is soil erosion index.

D. Soil Erosion Correlation Analysis

The elevation, slope, and water system distance influence the extent of human settlement and human activities. As a result, it influences the soil erosion phenomenon. Based on the land use data of Daning River Basin, spatial superposition analysis was adopted to calculate the soil erosion results of different influencing factors. The SEA, SEM, and SEI of different grades in each different influencing factor were counted.

The degree of soil erosion was produced by a combination of factors and the soil erosion was decided by the SEI magnitude. In this article, the SEI calculation model reported by Yang *et al.* [55] was used to obtain specific erosion characteristics. The larger SEI value represents the higher impact of the class. The more intense the soil erosion intensity, the more severe the erosion condition of the soil.

1) Correlation Between Distance From the River and Soil Erosion: Human activities have a greater impact on soil erosion. The intensity of human activities is higher in areas close to rivers. The Euclidean distance of the entire river basin was calculated according to the distance from the river and divided into six classes (0–1 km, 1–2 km, 2–3 km, 3–4 km, 4–5 km, >5 km). The spatial overlay was used to count the SEA, SEM and SEI for each class of distance from the river each year.

As shown in Fig. 5 SEA, the soil erosion in the 0–5 km area showed an increase followed by decreasing trend during 2008–2018. The soil erosion in the >5 km area showed a decreasing trend with time year by year. However, as a whole, soil erosion was mainly concentrated in the >5 km area, which was considered intensively. Considering the large difference in terrain height, steep slope, deep river valley, frequent occurrence of small geological disasters, and increased management efforts in the Daning River Basin, soil erosion in 2018 was significantly smaller than in 2008. Moreover, the ecological environment showed an improving trend.

As shown in Fig. 5 SEM, the erosion modulus changed during 2008–2018 and showed a decreasing trend. The change of erosion modulus in the area of 0-4km distance from the river

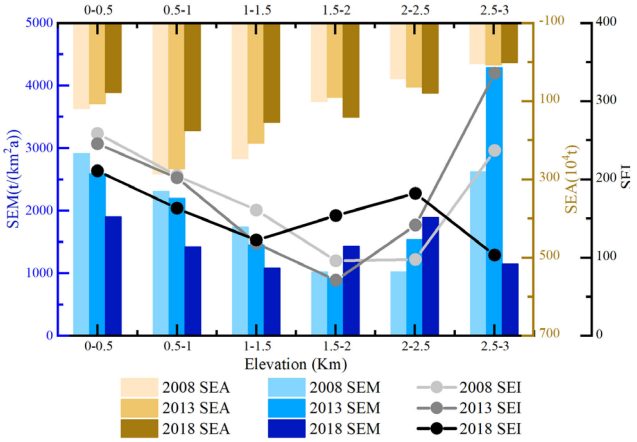

Fig. 6. SEA, SEM, and SEI with time at different elevations. Note: SEA is soil erosion amount, SEM is soil erosion modulus, and SEI is soil erosion index.

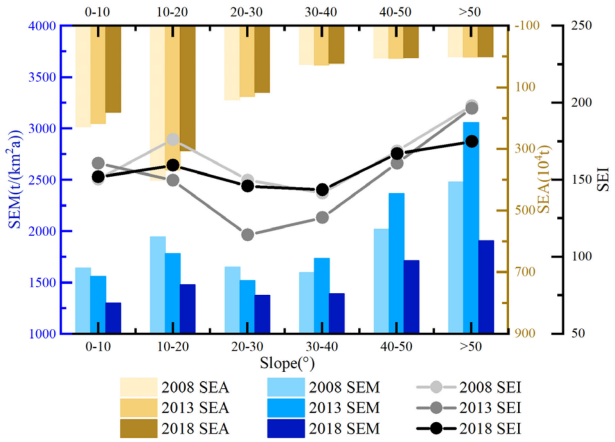

Fig. 7. SEA, SEM, and SEI with time for different slopes Note: SEA is soil erosion amount, SEM is soil erosion modulus, and SEI is soil erosion index.

showed a decreasing trend. The change of erosion modulus in the area of >4 km distance from the river demonstrated an increase followed by decreasing trend. The change of erosion modulus was larger between 0–2km from 2008–2018. Overall, the soil erosion in the 2–5 km range was in good condition, mainly due to the stable geological structure in this range and the good soil retention effect.

As shown in Fig. 5 SEI, during the period 2008–2018, the SEI was higher within the distance of 0–3 km from the river and the soil was susceptible to erosion. For the >3 km area from the river, the SEI was smaller and the area was more resistant to soil erosion. Therefore, it is necessary to focus on improving the soil erosion resistance in the near-river area. From a temporal perspective, the SEI of the 0–2 km area decreased year by year after ecological treatment and was subjected to lower erosion risk. Whereas, the SEI of the >2 km area increased in 2018 compared to 2013 and was less resistant to erosion.

2) Correlation Between Elevation and Soil Erosion: By analyzing the correlation between elevation and soil erosion, it was found that elevation controlled the distribution of vegetation and human activities. As a result, it had an obvious effect on soil erosion. Therefore, the SEM had a direct relationship with the elevation. The elevation of soil erosion in the Daning River Basin was divided into intervals of 500 m to obtain the relationship between the SEA, SEM, and SEI while having different elevation zones.

The graded elevation of the Daning River Basin was spatially overlaid with the results of soil erosion intensity grading. The SEI model was used to calculate the SEA, SEM, and SEI for each elevation band for each year. The relationship between different elevation zones and soil erosion data is shown in Fig. 6. Overall, the SEI was larger at each elevation, indicating the Daning River Basin to be influenced by elevation.

As shown in Fig. 6, the SEA and SEM trends were similar during 2008–2018. The SEA and SEM numbers in the 0–1.5 km area demonstrated a decreasing trend over time, which was attributed to the relatively flat topography of these slope sections, less change in vegetation cover and weaker rainwater scouring ability. The SEA and SEM in the 2–2.5 km area demonstrated an increasing trend year by year followed by serious damage by geological hazards, which was attributed to the large slope and geological fragility of the area. The 2.5–3 km area portrayed an increase followed by decreasing trend of SEA and SEM. The highest SEM in 2013 was mainly influenced by the unstable annual precipitation, large slope, and strong rainfall scouring ability, resulting in serious soil erosion. The higher the influence of gravity and precipitation on elevation, the greater the chance of soil erosion.

As shown in Fig. 6 SEI, during the period 2008–2018, the SEI was smaller in the 1–2.5 km area and was more resistant to soil erosion. The SEI was larger in the 0–1 km and 2.5–3 km areas and the soil was susceptible to erosion. The SEI change trend in 2008 and 2013 were similar in the 0–2 km area where the soil erosion resistance to erosion got stronger. The range of 2–3 km was increasingly vulnerable to erosion. For 2018, the area of 0–1 and 2–2.5 km SEI was larger and the soil was vulnerable to erosion.

3) Correlation Between Slope and Soil Erosion: The slope is one of the most influential factors in soil erosion results. The slope was equally spaced into six classes and superimposed with different classes of erosion intensity to obtain SEA, SEM, and SEI on different slope classes (see Fig. 7).

As shown in Fig. 7 SEA, the soil erosion in the 0–30° area showed a decreasing trend during 2008–2018 and the soil erosion in the >30° area showed an increase followed by a decreasing trend. Overall, soil erosion was mainly concentrated in the 10°–20° area. Due to the large difference in elevation, steep slope, and deep river valley in the Daning River Basin, small geological disasters occurred frequently. With increased management efforts, soil erosion in 2018 was significantly smaller than 2008 and the ecological environment showed an improving trend. The greater the possibility of soil erosion near the slope of 20°, the stronger the gravitational effect of soil downward. It indicates that the steeper the mountain area near the river, the greater the height drop and the more likely soil erosion occurs. The river has a stronger effect on soil erosion scouring and transporting, especially in the alternate rainy and dry seasons.

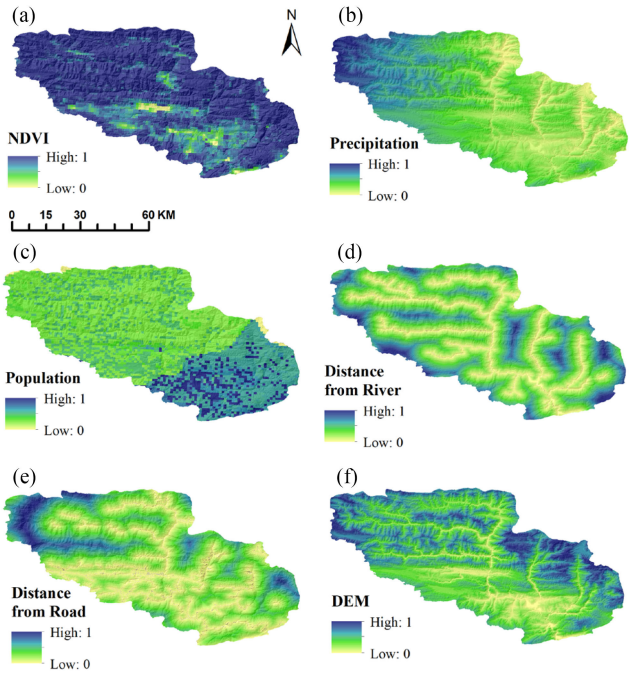

Fig. 8. Spatial distribution of normalized impact factors.

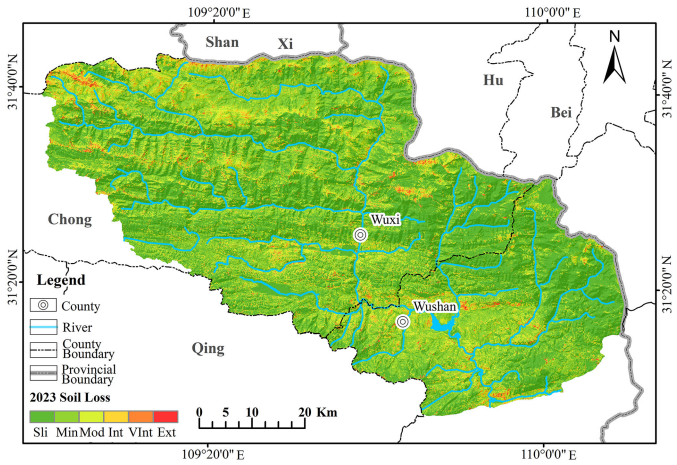

Fig. 9. Predicted soil erosion intensity in 2023. Note: Sli indicates that the soil erosion level is slight, Min indicates that the soil erosion level is minor, Int indicates that the soil erosion level is intense, VInt indicates that the soil erosion level is very intense, and Ext indicates that the soil erosion level is extreme.

TABLE VI
AREA COMPARISON OF SOIL EROSION INTENSITY DURING 2018–2023

Classes	2018(Year)		2023(Year)	
	EA (km^2)	AP (%)	EA (km^2)	AP (%)
Slight	2369.40	52.87	2271.27	50.74
Minor	1192.77	26.61	1253.46	28
Moderate	609.40	13.6	650.50	14.53
Intense	211.59	4.72	220.88	4.93
Very intense	89.07	1.99	78.61	1.76
Extreme	9.53	0.21	7.05	0.16
Total	4481.76	100	4481.76	100

Note: EA stands for erosion area and AP stands for area percentage.

As shown in Fig. 7 SEM, the SEM of the 0–30° area decreased with time during 2008–2018. The change in SEM of the >30° area increased and then decreased. The SEM was mainly concentrated between 0° and 30°. The SEM was influenced by a combination of factors such as human damage and topography. The SEM significantly varied until 2018.

As shown in Fig. 7 SEI, during 2008–2018, the SEI was higher in the area of 0–20° and >40° slopes and the soil was more vulnerable to erosion. The SEI was smaller in the area of 20°–40° slope and the area was more resistant to soil erosion. Therefore, it is necessary to increase the soil erosion resistance in the area vulnerable to erosion. From a temporal perspective, the SEI in 2013 was lower than 2008 and 2018.

E. Validation and Analysis of Prediction Results

Soil erosion in 2023 was simulated and predicted by the CA-ANN-Markov model using six driving factors (NDVI, precipitation, population, distance from the river, distance from the road and dem factor) (see Fig. 8). The simulation results of 2018 were verified by FoM to compare with the actual results. The FoM index was determined to be 0.149, indicating that the simulation results were reliable [52]. It shows that the prediction of future soil erosion by the CA-ANN-Markov model using the driving factors and parameters is useful, obtain soil erosion forecast results for 2023 (see Fig. 9).

As shown in Fig. 9, the spatial distribution of soil erosion in 2023 was similar to that in 2008, 2013, and 2018, with slight erosion being scattered in the Daning River Basin. Whereas, the minor, moderate, intense, and very intense erosion were distributed in the southern region. The slight erosion was mainly concentrated in the marginal areas of Daning River Basin, such as the areas near Houhe, Danyang, and Zhuxian Village, where the soil erosion was weak and the water as well as soil conservation effect was better. Minor erosion and moderate erosion were mainly distributed in the vicinity of Datong, Jianlou, Yixi, and Qiyang Village. The erosion near Baiyun, Dachang, and Huatai Village was comparatively critical. The erosion continued to be unabated from 2008 to 2023 due to rainfall erosion and geographical location. The soil erosion and scouring phenomenon were serious due to the large short-lived rainstorm near Huatai Village, abundant rainfall and strong scouring ability. The combination of rainfall and terrain factors in local areas resulted in the reduction of soil suction, which lead to soil erosion in the Daning River Basin. It also induced shallow soil landslides in serious areas. Soil erosion in areas with frequent human activities was more serious because of rainfall scouring and soil erosion occurred frequently.

Comparing the changes in the area between different intensities of soil erosion in 2018 and 2023 (see Table VI) from the perspective of the area and the percentage of slight, the minor and moderate erosion in 2023 was found to be higher. The percentage of intense, very intense, and extreme erosion was smaller, which was similar to the percentage of area covered by different erosion intensities in 2018. The change in the area and the percentage of area occupied by slight erosion during 2018–2023 of the total area decreased from 52.87% to 50.74%.

The area occupied by slight erosion in the future Daning River Basin erosion increased slightly from 26.61% to 28%. The area of moderate erosion had a small increase from 13.6% to 14.53%. The area of intense erosion had a small increase from 4.72% to 4.93%. There was a corresponding decrease in both very intense and extreme erosion in the Daning River Basin. The very intense erosion decreased from 1.99% to 1.76% and extreme erosion decreased from 0.21% to 0.16%.

IV. Discussion

This study calculated and inverted the current situation and future trends of soil erosion in the Daning River Basin while providing new ideas for soil erosion restoration and control.

In terms of soil erosion change characteristics, this study showed that the soil erosion situation from 2008 to 2013 was dominated by minor erosion. Moreover, the soil SEM decreased and the soil erosion condition showed an improving trend. The conclusions of this study were consistent with the results, SEM changes, spatial and temporal changes of soil erosion reported by other scholars [56]–[60], which indicated the credibility of this study.

The RUSLE model having well-established model parameters (P, C, K, R, and LS) was selected in this study followed by parameter selection and calculation methods based on previous reports [13], [49], [50]. The CA-ANN-Markov parameters were also determined with reference to previous studies [61]–[63]. Parametric deterministic analysis was also conducted and the driving force of each predictor was analyzed using the geographic probe. The higher contribution was attributed to DEM, distance from water and NDVI. The driving force of the interaction of both factors was higher than that of the single factor, where q (distance from river $\cap$ dem) was 19% and q (distance from river $\cap$ NDVI) was 16%. Risk detection showed that the predictors positively correlated with soil erosion which included road distance, NDVI, DEM, and precipitation. The negatively correlated included population density and watershed distance. Therefore, these six factors were selected in this study. With higher elevation, lower the population density, higher vegetation, higher NDVI, and farther distance from the road, the soil erosion in the Daning River Basin is reduced. Areas close to the watershed have better water conservation, dense vegetation growth, and better soil and water conservation, whereas areas far from the watershed have poor water conservation and sparse ground cover soils. Therefore, the area far from the watershed is more susceptible to erosion.

In terms of prediction models, the 2018 CA-ANN-Markov simulation results were validated with the RUSLE results while resulting in an FoM index of 0.149, which indicated that the simulation results were reliable [52], Xing [63], and Ran [64] also analyzed the accuracy of the ANN-CA-Markov model, resulting in higher accuracy outcome (Kappa coefficient 0.9836) than the KarstCA model, CLUE-S model, CA-Markov model, and MCE-CA-Markov model, which proved the accuracy and feasibility of the model for the prediction of soil erosion intensity.

In terms of future control measures, the effect of soil erosion management in the Daning River Basin was considered. The soil erosion in 2008 was significantly greater than 2018. Based on the predicted results for 2023, soil erosion demonstrated an improving trend. However, there was still room for improvement from the expected target. Therefore the zoning treatment is necessary. For soil erosion in northwest China, which is dominated by mild erosion and moderate erosion, ecological restoration can be used to gradually restore a stable soil environment. For areas with severe soil erosion in the Daning River Basin, comprehensive treatment by afforestation, engineering construction, and biological control should be actively carried out. For example, the areas with large slopes and thin soil should be returned to the forest. The barren hills and wildlands with poor vegetation should be planted with trees while turning into greener projects.

Based on this study, from data selection to its analysis after calculating the results through the methodological model, some problems need to be improved:

1) the time window of future research can be further refined, such as the monthly and quarterly relationships between erosion results and impact factors can be considered;
2) the variable factors affecting soil erosion can be further deepened and expanded;
3) soil erosion in mountainous areas of complex watersheds is difficult to be explained by single-factor or two-factor predictor variables and may be subjected to the synergistic effects of multiple factors, whose specific mechanisms of action are still unclear and is the next research direction for the author.

V. Conclusion

Soil erosion in the Daning River Basin is influenced by multiple factors and has significant spatial and temporal variation characteristics. Combining GIS and RS technology to pre-process the data of Daning River Basin, the RUSLE model was constructed to simulate soil erosion in the study area. Using the calculation model of comprehensive SEI, the quantitative evaluation was carried out while considering the soil erosion from geomorphology, hydroclimate, and natural environment. The CA-ANN-Markov model was used to predict the soil erosion distribution in 2023 and the results provided scientific and technical support for soil erosion management in the Daning River Basin. The specific conclusions are as follows.

1) The spatial and temporal variations of different soil erosion intensities were found to be different. The area of soil erosion intensity of slight, very intense, and extreme erosion showed a fluctuating trend including increase and then decrease. The area of minor erosion, moderate erosion and intense erosion first decreased and then increased.
2) Soil erosion was correlated differently with the influencing factors. The correlation analysis of distance from the river, elevation, and slope with SEA, SEM, and SEI showed that SEA was the largest in the area with a >5 km distance from the river, elevation in the range of 0.5–1.5 km, and slope in the range of 10°–20°. The SEM and SEI were the largest in the area with a distance of 0–1 km from the river, elevation in the range of 2.5–3 km, and slope in the range of $>50°$.
3) The CA-ANN-Markov model predicted soil erosion in 2023. Soil erosion trends from 2018 to 2023 were generally consistent with those from 2008 to 2013. Slight erosion was predominant throughout the region. The minor, moderate, intense, and very intense erosion accounted for a small percentage and were geospatially limited.

REFERENCES

[1] W. Sun, Q. Shao, J. Liu, and J. Zhang, "Assessing the effects of land use and topography on soil erosion on the Loess Plateau in China," *CATENA*, vol. 121, no. 1, pp. 151–163, 2014, doi: 10.1016/j.catena.2014.05.009.

[2] M. M. Wei, S. H. Fu, and B. Y. Liu, " Quantitative research of water erosion on the Qinghai-Tibet Plateau," *Adv. Earth Sci.*, vol. 36, no. 7, pp. 740–752, 2021.

[3] M. Liu and G. L. Han, "Distribution of soil nutrients and erodibility factor under different soil types in an erosion region of Southeast China," *Peer J.*, vol. 16, no. 9, 2021, Art. no. e11630, doi: 10.7717/PEERJ.11630.

[4] T. Schmid *et al.*, "Characterization of soil erosion indicators using hyperspectral data from a Mediterranean rainfed cultivated region," *IEEE J. Sel. Topics Appl. Earth Observ. Remote Sens.*, vol. 9, no. 2, pp. 845–860, Feb. 2016, doi: 10.1109/JSTARS.2015.2462125.

[5] M. K. Luo *et al.*, "Effect of river-lake connectivity on heavy metal diffusion and source identification of heavy metals in the middle and lower reaches of the Yangtze River," *J. Hazardous Mater.*, vol. 416, 2021, Art. no. 125818, doi: 10.1016/J.JHAZMAT.2021.125818.

[6] Y. X. Wang, G. H. Liu, Z. H. Zhao, C. S. Wu, and B. W. Yu, " Using soil erosion to locate nonpoint source pollution risks in coastal zones: A case study in the Yellow River Delta, China," *Environ. Pollut.*, vol. 283, 2021, Art. no. 117117, doi: 10.1016/J.ENVPOL.2021.117117.

[7] J. X. Chen, D. P. Yue, J. P. Wang, S. Shang, and M. C. Ma, "Development and application of a GIS calculation system for soil erosion," *J. Northwest Forestry Univ.*, vol. 31, no. 1, pp. 206–213, 2016.

[8] Y. D. Wang, W. Ouyang, Y. H. Zhang, C. Y. Lin, M. C. He, and P. T. Wang, "Quantify phosphorus transport distinction of different reaches to estuary under long-term anthropogenic perturbation," *Sci. Total Environ.*, vol. 780, 2021, Art. no. 146647, doi: 10.1016/J.SCITOTENV.2021.146647.

[9] H. J. Zhang and J. H. Cheng, *Soil Erosion Principle*. Beijing, China: China Sci. Publishing Media, 2014, p. 3.

[10] Q. F. Gao, S. Guo, S. M. Song, Z. X. Que, and T. X. Li, "RUSLE model based-on quantitative estimation and spatial characteristics study on regional," *Water Resour. Hydropower Eng.*, vol. 49, no. 6, pp. 214–223, 2018, doi: 10.13928/j.cnki.wrahe.2018.06.030.

[11] D. C. Flanagan, J. C. Ascough, M. A. Nearing, and J. M. Laflen, "The Water Erosion Prediction Project (WEPP) model," in *Landscape Erosion and Evolution Modeling*, R. S. Harmon and W. W. Doe, Eds. Boston, MA, USA: Springer, 2001, doi: 10.1007/978-1-4615-0575-4.

[12] R. P. C. Morgan *et al.*, "The European Soil Erosion Model (EUROSEM): A dynamic approach for predicting sediment transport from fields and small catchments," *Earth Surf. Processes Landforms*, vol. 23, no. 6, pp. 527–544, 1998, doi: 10.1002/(SICI)1096-9837(199806)23:6<527::AID-ESP868>3.0.CO;2-5.

[13] W. H. Wischmeier, C. B. Johnson, and B. V. Cross, "A soil erodibility nomograph for farmland and construction sites," *J. Soil Water Conserv.*, vol. 26, pp. 189–193, 1971, doi: 10.2307/3896643.

[14] J. R. Williams, "Sediment-yield prediction with universal equation using runoff energy factor," *Environ. Sci.*, vol. 40, 1975, Art. no. 244.

[15] K. G. Renard, G. R. Foster, G. A. Weesies, and J. P. Porter, "RUSLE-revised universal soil loss equation," *J. Soil Water Conserv.*, vol. 46, no. 1, pp. 30–35, 1991, doi: 10.1002/9781444328455.ch8.

[16] L. M. Risse, M. A. Nearing, J. M. Laflen, and A. D. Nicks, "Error assessment in the universal soil loss equation," *Soil Sci. Soc. Amer. J.*, vol. 57, no. 3, pp. 825–833, 1993, doi: 10.2136/sssaj1993.03615995005700030032x.

[17] J. F. Rapp, V. L. Lopes, and K. G. Renard, "Comparing soil erosion estimates from RUSLE and USLE on natural runoff plots," in *Soil Erosion Research for the 21st Century*, J. C. Ascough and D. C. Flanagan, Eds. St. Joseph, MI, USA: ASAE, 2001, pp. 24–27.

[18] C. Alewell, P. Borrelli, K. Meusburger, and P. Panagos, "Using the USLE: Chances, challenges and limitations of soil erosion modelling," *Int. Soil Water Conserv. Res.*, vol. 7, no. 3, pp. 203–225, 2019, doi: 10.1016/j.iswcr.2019.05.004.

[19] K. G. Renard, G. R. Foster, D. C. Yoder, and D. K. McCool, "RUSLE revisited: Status, questions, answers, and the future," *J. Soil Water Conserv.*, vol. 49, no. 3, pp. 213–220, 1994, doi: 10.1111/j.2044-8279.1937.tb03176.x.

[20] P. Tian *et al.*, "Soil erosion assessment by RUSLE with improved P factor and its validation: Case study on mountainous and hilly areas of Hubei Province, China," *Int. Soil Water Conserv.*, vol. 9, no. 3, pp. 433–444, 2021, doi: 10.1016/J.ISWCR.2021.04.007.

[21] Y. Bai and H. F. Cui, "An improved vegetation cover and management factor for RUSLE model in prediction of soil erosion," *Environ. Sci. Pollut. Res.*, vol. 28, pp. 21132–21144, 2021, doi: 10.1007/S11356-020-11820-X.

[22] Y. Xiao *et al.*, "Spatial-temporal evolution patterns of soil erosion in the Yellow River Basin from 1990 to 2015: Impacts of natural factors and land use change," *Geomatics Natural Hazards Risk*, vol. 12, no. 1, pp. 103–122, 2020, doi: 10.1080/19475705.2020.1861112.

[23] C. R. D. Mello, L. D. Norton, L. C. Pinto, S. Beskow, and N. Curi, "Agricultural watershed modeling: A review for hydrology and soil erosion processes," *Ciência e Agrotecnologia*, vol. 40, no. 1, pp. 7–25. 2016, doi: 10.1590/S1413-70542016000100001.

[24] J. Wang, H. Qian, P. Zhou, and Q. H. Gong, "Test of the RUSLE and key influencing factors using GIS and probability methods: A case study in Nanling National Nature Reserve, South China," *Adv. Civil Eng.*, vol. 2019, pp. 1–15, 2019, doi: 10.1155/2019/7129639.

[25] X. Y. Zhu, R. Z. Zhang, and X. W. Sun, "Spatiotemporal dynamics of soil erosion in the ecotone between the Loess Plateau and Western Qinling Mountains based on RUSLE modeling, GIS, and remote sensing," *Arab. J. Geosci.*, vol. 14, no. 1, 2021, doi: 10.1007/S12517-020-06329-Z.

[26] A. Tairi, A. Elmouden, L. Bouchaou, and M. Aboulouafa, "Mapping soil erosion-prone sites through GIS and remote sensing for the Tifnout Askaoun watershed, southern Morocco," *Arabian J. Geosci.*, vol. 14, no. 9, 2021, Art. no. 811, doi: 10.1007/S12517-021-07009-2.

[27] L. Tsegaye and R. Bharti, "Soil erosion and sediment yield assessment using RUSLE and GIS-based approach in Anjeb watershed, Northwest Ethiopia," *SN Appl. Sci.*, vol. 3, 2021, Art. no. 582, doi: 10.1007/S42452-021-04564-X.

[28] G. H. Fang, T. Yuan, Y. Zhang, X. Wen, and R. J. Lin, "Integrated study on soil erosion using RUSLE and GIS in Yangtze River Basin of Jiangsu Province (China)," *Arabian J. Geosci.*, vol. 12, no. 5, 2019, Art. no. 173, doi: 10.1007/s12517-019-4331-2.

[29] J. L. Li, R. H. Sun, M. Q. Xiong, and G. C. Yang, "Estimation of soil erosion based on the RUSLE model in China," *Acta Ecologica Sinica*, vol. 40, no. 10, pp. 3473–3485, 2020.

[30] E. Salifu, W. A. Agyare, N. Kyei-Baffour, and G. Dumedah, "Estimation of soil erosion in three northern regions of Ghana using RUSLE in GIS environment," *Int. J. Appl. Geospatial Res.*, vol. 12, no. 2, pp. 1–19, 2021, doi: 10.4018/IJAGR.2021040101.

[31] M. Masroor *et al.*, "Analysing the relationship between drought and soil erosion using vegetation health index and RUSLE models in Godavari middle sub-basin, India," *Geosci. Front.*, vol. 13, no. 2, pp. 27–39, 2022, doi: 10.1016/j.gsf.2021.101312.

[32] L. Zhao, J. Yang, C. Li, Y. T. Ge, and Z. L. Han, "Progress on geographic cellular automata model," *Scientia Geographica Sinica*, vol. 36, no. 8, pp. 1190–1196, 2016, doi: 10.13249/j.cnki.sgs.2016.08.009.

[33] T. T. Dong, L. J. You, and Z. X. Zhang, "A study on spacetime evolution of soil erosion based on ANN-CA model," *J. Geo-Inf. Sci.*, vol. 1, no. 1, pp. 132–138, 2009.

[34] Y. X. Pu, R. H. Ma, Y. Ge, and X. Y. Huang, "Spatial-Temporal dynamics of Jiangsu regional convergence with spatial Markov chains approach," *Chin. Geograph. Sci.*, vol. 5, pp. 817–826, 2005.

[35] J. T. Zhao, Y. X. Ma, Y. Shi, S. S. Hao, and X. Y. Ma, "Prediction of soil erosion evolution in counties in the Loess hilly region based on ANN-CA model," *Sci. Soil Water Conserv.*, vol. 19, no. 6, pp. 60–68, 2021, doi: 10.16843/j.sswc.2021.06.008.

[36] Y. K. Li, S. Y. Yao, F. Yan, L. J. Chen, and Y. H. Qi, "Based on improved automata-Markov model-based simulation and prediction on evolution of land use pattern: A case of Xinyu City," *Water Resour. Hydropower Eng.*, vol. 53, no. 4, pp. 71–83, 2022, doi: 10.13928/j.cnki.wrahe.2022.04.006.

[37] Y. H. Zhao, L. Liu, S. Z. Kang, Y. Ao, L. Han, and C. Q. Ma, "Quantitative analysis of factors influencing spatial distribution of soil erosion based on geo-detector model under diverse geomorphological types," *Land*, vol. 10, no. 6, 2021, Art. no. 604, doi: 10.3390/LAND10060604.

[38] Y. Xiao, Q. Xiao, Q. L. Xiong, and Z. P. Yang, "Effects of ecological restoration measures on soil erosion risk in the Three Gorges Reservoir area since the 1980s," *Geohealth*, vol. 4, no. 12, 2020, Art. no. e2020GH000274, doi: 10.1029/2020GH000274.

[39] L. Chu, T. C. Sun, T. W. Wang, Z. X. Li, and C. F. Cai, "Temporal and spatial heterogeneity of soil erosion and a quantitative analysis of its determinants in the Three Gorges Reservoir area, China," *Int. J. Environ. Res. Public Health*, vol. 17, no. 22, 2020, Art. no. 8486, doi: 10.3390/ijerph17228486.

[40] Y. W. Deng, G. Lin, and H. P. Zeng, "Simulation research on temporal and spatial changes of land use in Tianjin municipality based on CA-Markov model," *J. Tianjin Chengjian Univ.*, vol. 27, no. 6, pp. 387–395, 2021, doi: 10.19479/j.2095-719x.2106387.

[41] M. T. U. Rahman *et al.*, "Temporal dynamics of land use/land cover change and its prediction using CA-ANN model for southwestern coastal Bangladesh," *Environ. Monit. Assess.*, vol. 189, no. 11, 2017, Art. no. 565, doi: 10.1007/s10661-017-6272-0.

[42] Q. L. Xu, Q. Wang, J. Liu, and L. Hong, "Simulation of land-use changes using the partitioned ANN-CA model and considering the influence of land-use change frequency," *ISPRS Int. J. Geo-Inf.*, vol. 10, no. 5, 2021, Art. no. 346, doi: 10.3390/IJGI10050346.
[43] *National Soil and Water Conservation Bulletin: 2020*, Ministry of Water Resources of the People's Republic of China, Beijing, China, 2020.
[44] N. F. Fang, "Rainfall, runoff and sediment delivery relationships associated with soil conservation measures at the small watershed level," Ph.D. dissertation, Dept. Resour. Environ. Inf. Eng., Huazhong Agricultural Univ., Wuhan, China, 2012.
[45] A. Elnashar, H. W. Zeng, B. F. Wu, A. A. Fanta, M. Nabil, and R. Duerler, "Soil erosion assessment in the Blue Nile Basin driven by a novel RUSLE-GEE framework," *Sci. Total Environ.*, vol. 793, 2021, Art. no. 148466, doi: 10.1016/J.SCITOTENV.2021.148466.
[46] M. Kumar, A. P. Sahu, N. Sahoo, S. S. Dash, S. K. Raul, and B. Panigrahi, "Global-scale application of the RUSLE model: A comprehensive review," *Hydrol. Sci. J.*, vol. 67, no. 5, pp. 806–830, 2022, doi: 10.1080/02626667.2021.2020277.
[47] D. S. Lu, M. Batistella, and E. Moran, "Multitemporal spectral mixture analysis for amazonian land-cover change detection," *Can. J. Remote Sens.*, vol. 30, no. 1, pp. 87–100, 2004, doi: 10.5589/m03-055.
[48] W. H. Wischmeier, C. B. Johnson, and B. V. Cross, "A soil erodibility nomograph for farmland and construction sites," *J. Soil Water Conserv.*, no. 26, pp. 189–193, 1971, doi: 10.2307/3896643.
[49] B. Y. Liu, Y. Xie, and K. L. Zhang, *Soil Erosion Forecasting Model*. Beijing, China: Sci. Technol. China Press, 2001, pp. 101–110.
[50] K. L. Zhang, Y. M. Cai, B. Y. Liu, and W. Y. Peng, "Fluctuation of soil erodibility due to rainfall intensity," *Acta Geographica Sinica*, vol. 6, pp. 673–681, 2001.
[51] Y. Yao *et al.*, "Simulating urban land-use changes at a large scale by integrating dynamic land parcel subdivision and vector-based cellular automata," *Int. J. Geogr. Inf. Sci.*, vol. 31, no. 12, pp. 2452–2479, 2017, doi: 10.1080/13658816.2017.1360494.
[52] X. P. Liu *et al.*, "A future land use simulation model (FLUS) for simulating multiple land use scenarios by coupling human and natural effects," *Landscape Urban Plan.*, vol. 168, pp. 94–116, 2017, doi: 10.1016/j.landurbplan.2017.09.019.
[53] X. L. Wang and Y. M. Bao, "Study on the methods of land use dynamic change research," *Prog. Geogr.*, vol. 1, pp. 83–89, 1999.
[54] *Standards for Classification and Graduation Soil Erosion: SL190-2007[S]*, Ministry of Water Resources of the People's Republic of China, Beijing, China, 2007.
[55] C. J. Yang, J. Y. Liu, Z. X. Zhang, Q. B. Zhou, and X. L. Zhao, "Analysis of features of soil erosion under different slope supported based on GIS," *J. Soil Water Conserv.*, vol. 12, no. 6, pp. 46–49, 2002, doi: 10.13870/j.cnki.stbcxb.2002.06.014.
[56] K. X. Yang, Q. Liu, X. H. Li, Y. R. Lu, L. Liu, and W. Z. Song, "Analysis of soil erosion and fractional vegetation cover change in the Three Gorges Reservoir area," *J. Beijing Normal Univ. (Natural Sci.)*, vol. 57, no. 5, pp. 631–638, 2021, doi: 10.12202/j.0476-0301.2021049.
[57] X. M. Zhang, "Land use change and effects of soil conservation in the Daning River watershed," M.S. thesis, School Geography Tourism, Chongqing Normal Univ., Chongqing, China, 2015.
[58] R. K. Li, Y. B. Li, W. Wen, Y. L. Zhou, X. Y. Liang, and Y. H. Liu, "Study on the temporal and spatial variation of soil erosion intensity in a typical watersheds of the Three Gorges Reservoir area from 1988 to 2015A case based on the Daning and Meixi River watersheds," *Acta Ecologica Sinica*, vol. 38, no. 17, pp. 6243–6257, 2018, doi: 10.5846/stxb201706071040.
[59] Y. L. Feng, "Research on characteristics of ecological threat and ecological restoration of Caotang River Basin three gorges reservoir area," M.S. thesis, School Geography Tourism, Chongqing Normal Univ., Chongqing, China, 2012.
[60] W. Liu, W. An, M. Yang, and J. F. MA, "Runoff and sediment yield modeling and soil erosion analysis in Daning River watershed in Three Gorges Reservoir region based on SWAT model," *J. Soil Water Conserv.*, vol. 30, no. 4, pp. 49–56, 2016, doi: 10.13870/j.cnki.stbcxb.2016.04.009.
[61] L. D. Zheng, "Spatial and temporal pattern and evolution simulation of the soil erosion of southern red soil region based on ANN-CA," M.S. thesis, School Geographical Sci., Fujian Normal Univ., Fujian, China, 2012.
[62] C. Qin, "Research on the evolution of rural settlement space layout based on model of ANN-CA," M.S. thesis, China Univ. Mining Technol., Xuzhou, China, 2020.
[63] R. S. Xing, "Research on ecological space pattern simulation based on ANN-CA-Markov and site condition quality evaluation—A case study of Wanzhou district," M.S. thesis, School Environ. Resour., Chongqing Univ. Technol. Ind., Chongqing, China, 2020.
[64] G. X. Ran, "Analysis and prediction of soil erosion in li county," M.S. thesis, Dept. Surveying Mapping Eng., Chengdu Univ. Technol., Chengdu, China, 2019.

Wenqian Bai received the B.S. degree in engineering from Shandong Agricultural and Engineering University, Jinan, China, in 2018, and the M.S. degree in cartography and geographic information systems in 2021 from Chengdu University of Technology, Chengdu, China, where she is currently working toward the Ph.D. degree in geological resources and geological engineering.

Her research interests include remote sensing of resources and environment, soil erosion, and net primary productivity.

Huiru Hu received the M.S. degree in cartography and geographic information systems from Chengdu University of Technology, Chengdu, China, in 2021.

Her research interests include remote sensing of resources and environment, soil erosion, and land use change.

Li He received the B.S. degree in geology from Chengdu University of Technology, Chengdu, China, in 2014, and the direct Ph.D. degree in geography from the Institute of Mountain Hazards and Environment, Chengdu, China, in 2020.

She is currently a Lecturer with the College of Tourism and Urban-Rural Planning, Chengdu University of Technology, Chengdu, China. Her research interests include remote sensing of resources and environment.

Zhengwei He received the B.S. degree in geology and the M.S. degree in geology from Jilin University, Jilin, China, in 1989 and 1992, respectively, and the Ph.D. degree in geological resources and geological engineering from Chengdu University of Technology, Chengdu, China, in 1998.

He is currently a Professor with the College of Earth Sciences, Chengdu University of Technology. His research interests include remote sensing of resources and environment, metallogenic regularity and metallogenic prediction, geographic information systems, ecological environment evaluation, territorial spatial planning, land use, and remote sensing, machine learning.

Yang Zhao received the M.S. degree in physical geography from Chengdu University of Technology, Chengdu, China, in 2018.

His research interests include remote sensing of resources and territorial spatial planning, land use, remote sensing, and machine learning.